Appl Microbiol Biotechnol (2016) 100:8523–8535
DOI 10.1007/s00253-016-7653-y

ENVIRONMENTAL BIOTECHNOLOGY

Characterization of the microbial community composition and the distribution of Fe-metabolizing bacteria in a creek contaminated by acid mine drainage

Weimin Sun[1,2,3] · **Enzong Xiao**[1,4] · **Valdis Krumins**[5] · **Yiran Dong**[6] · **Tangfu Xiao**[1,7] · **Zengping Ning**[1] · **Haiyan Chen**[1,4] · **Qingxiang Xiao**[1,4]

Received: 1 May 2016 / Revised: 23 May 2016 / Accepted: 26 May 2016 / Published online: 9 June 2016

Abstract A small watershed heavily contaminated by long-term acid mine drainage (AMD) from an upstream abandoned coal mine was selected to study the microbial community developed in such extreme system. The watershed consists of AMD-contaminated creek, adjacent contaminated soils, and a small cascade aeration unit constructed downstream, which provide an excellent contaminated site to study the microbial response in diverse extreme AMD-polluted environments. The results showed that the innate microbial communities were dominated by acidophilic bacteria, especially acidophilic Fe-metabolizing bacteria, suggesting that Fe and pH are the primary environmental factors in governing the indigenous microbial communities. The distribution of Fe-metabolizing bacteria showed distinct site-specific patterns. A pronounced shift from diverse communities in the upstream to *Proteobacteria*-dominated communities in the downstream was observed in the ecosystem. This location-specific trend was more apparent at genus level. In the upstream samples (sampling sites just below the coal mining adit), a number of Fe(II)-oxidizing bacteria such as *Alicyclobacillus* spp., *Metallibacterium* spp., and *Acidithrix* spp. were dominant, while *Halomonas* spp. were the major Fe(II)-oxidizing bacteria observed in downstream samples. Additionally, *Acidiphilium*, an Fe(III)-reducing bacterium, was enriched in the upstream samples, while *Shewanella* spp. were the dominant Fe(III)-reducing bacteria in downstream samples. Further investigation using linear discriminant analysis (LDA) effect size (LEfSe), principal coordinate analysis (PCoA), and unweighted pair group method with arithmetic mean (UPGMA) clustering confirmed the difference of microbial communities between upstream and downstream samples. Canonical correspondence analysis (CCA) and Spearman's rank correlation indicate that total organic carbon (TOC) content is the primary environmental parameter in structuring the indigenous microbial communities, suggesting that the microbial communities are shaped by three major environmental parameters (i.e., Fe, pH, and TOC). These findings were beneficial to a better understanding of natural attenuation of AMD.

Keywords Fe(II)-oxidizing bacteria · Fe(III)-reducing bacteria · Fe cycling · High-throughput sequencing

Weimin Sun and Enzong Xiao contributed equally to this work.

Electronic supplementary material The online version of this article (doi:10.1007/s00253-016-7653-y) contains supplementary material, which is available to authorized users.

✉ Tangfu Xiao
xiaotangfu@vip.gyig.ac.cn

[1] State Key Laboratory of Environmental Geochemistry, Chinese Academy of Sciences, 99 Lincheng Road West, Guiyang 550081, Guizhou Province, People's Republic of China

[2] Department of Biochemistry and Microbiology, Rutgers University, New Brunswick, NJ 08901, USA

[3] Guangdong Institute of Eco-environment and Soil Sciences, Guangzhou 510650, China

[4] University of Chinese Academy of Sciences, Beijing 100049, China

[5] Department of Environmental Sciences, Rutgers University, New Brunswick, NJ 08901, USA

[6] Department of Geology, University of Illinois-Urbana Champaign, Urbana, IL 61801, USA

[7] Innovation Center and Key Laboratory of Waters Safety & Protection in the Pearl River Delta, Ministry of Education, Guangzhou University, Guangzhou 510006, China

Introduction

Acid mine drainage (AMD) originates from oxidative dissolution of sulfur-containing minerals (e.g., pyrite (FeS_2)) due to metal ores and/or coal mining (Johnson 2003). The chemical reactions leading to the formation of AMD have been described extensively elsewhere (for details, please see reviews (Baker and Banfield 2003; Hallberg 2010; Johnson and Hallberg 2005)). In general, AMD is characterized by low pH and elevated concentrations of metals and metalloids. This extreme environment is toxic to most prokaryotic and eukaryotic organisms, posing a severe threat to both aquatic and terrestrial ecosystems (Johnson and Hallberg 2003). However, some microorganisms are reported to thrive in AMD-impacted environments, mediating both the formation and remediation of AMD, and influence the morphology and chemistry of minerals. For example, Fe(II)-oxidizing bacteria (FeOB) increase the rate of oxidative dissolution of pyrite and play a major role in the genesis of AMD when pH < 4 (Johnson and Hallberg 2003). These moderate or acidophilic mineral-oxidizing bacteria are distributed in AMD sites worldwide, and the most frequently encountered bacteria are *Thiobacillus ferrooxidans* (Rojas et al. 1995) and *Leptospirillum ferrooxidans* (Das and Ayyappan 1999; Rojas-Chapana and Tributsch 2004). In contrast, the reduction of sulfate (SO_4^{2-}) and Fe(III) generates alkalinity, leading to increases in pH and immobilization of metal(loid)s (Vile and Wieder 1993). Therefore, the sulfate-reducing bacteria (SRB) or Fe(III)-reducing bacteria (FeRB) are potentially significant in AMD remediation (Johnson 1995; Johnson and Hallberg 2003). Although biotic Fe(II) oxidation is the major cause of AMD genesis, precipitation of Fe(III) compounds is also a major metal immobilization process in some engineered AMD treatment systems such as wetlands and bioreactors (Johnson and Hallberg 2005). In light of the variety of documented microbial processes, there is great potential to harness these microbes to treat AMD. However, our current understanding of the indigenous microbial communities that catalyze different biological processes under in situ AMD conditions is relatively limited.

In order to elucidate the microorganisms inhabiting in AMD environments, an AMD-contaminated site located in the southwest coal basin (SCB) in central Guizhou, Southwest China, was selected as a study site. The hydrothermal conditions (warm temperature and high annual precipitation) in the SCB favor the formation of AMD, which has caused widespread environmental problems in this region. Numerous AMD creeks in this region discharge polluted mine waters into downstream rivers and reservoirs. Here, these AMD runoffs contaminated the drinking water sources for Guiyang City, the capital of Guizhou Province, with more than 500,000 inhabitants potentially exposed (Sun et al. 2015a, b). We selected one of the many AMD-contaminated creeks, Huaxi Creek, to study the dynamics and metabolic potential of microbial communities in response to long-term AMD contamination. This study site allowed for investigation of both natural (unmodified AMD impacted stream) and engineered habitats (constructed four-cell cascade aeration units (AUs) downstream of the creek) (Fig. 1). The AUs were constructed to test the feasibility of in situ cascade oxidation for alleviating AMD contamination. Orange Fe-rich sediments appeared in these AUs after operating for a short time (less than 1.5 years). As for the natural habitats, orange mats are present in the main course of the creek after long-term AMD runoff (more than 15 years). In addition, soils adjacent to the creek were stained by repeated flooding of AMD and thus were selected for microbial community analysis. In the present study, we sampled orange mats from the main course of the creek, surrounding contaminated soils, and sediments from the cascade AU. We aimed to (i) characterize the microbial community composition in both "natural" and engineered ecosystems; (ii) compare the microbial community from different environmental samples including mats, sediments, and soils; and (iii) correlate the microbial community with

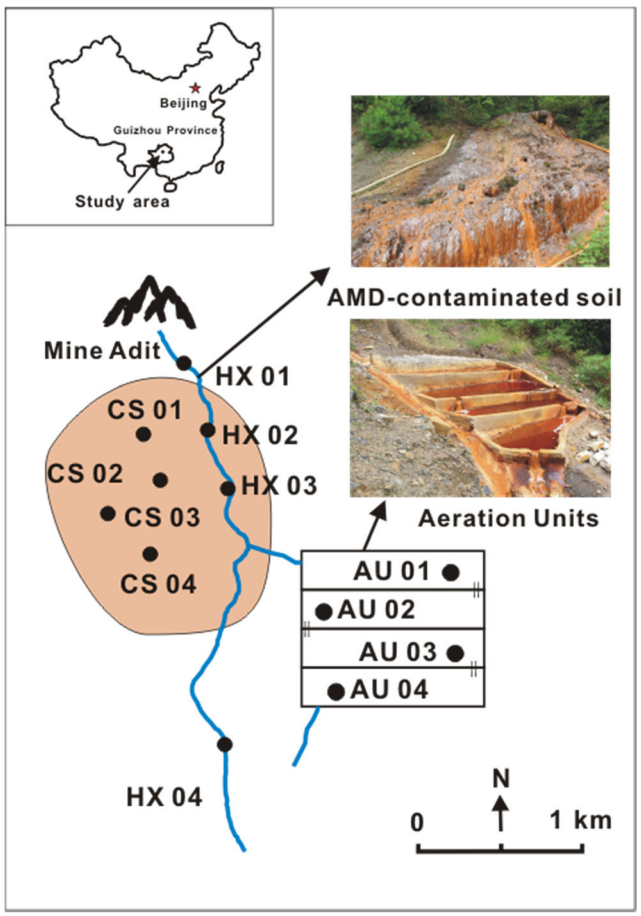

Fig. 1 Map of the AMD-contaminated watershed. Four creek mats were named as HX01–HX04; four contaminated soils were named as CS01–CS04; four sediments of aeration units were named as AU01–AU04

geochemical parameters and determine the interplay between microorganisms and their habitats.

Materials and methods

Sample collection

Twelve solid samples and seven water samples were collected at different locations along the Huaxi AMD creek in June, 2015. As illustrated by Fig. 1, samples HX01 to HX04 were collected from orange mats. Four samples (AU01–AU04) were collected from the sediments of AU, and four samples (CS01–CS04) were collected from the contaminated soils. Specifically, CS01 to CS04 were collected from the top soils (0–5 cm). Approximately 100 g of solid sample was collected per site. Solid samples from each site were pooled, homogenized, placed in sterile 50-ml tubes, and immediately stored at −20 °C until further molecular analysis.

Geochemical parameters in the water

Water quality parameters including pH and redox potential (Eh) were measured onsite by a calibrated HACH HQ30d pH meter (HACH, Loveland, CO, USA). Major and trace elements in water samples were measured by inductively coupled plasma-optical emission spectrometry (ICP-OES) (Vista MPX, Varian, USA) and inductively coupled plasma mass spectrometry (ICP-MS) (Agilent, 7700x, Santa Clara, CA, USA), respectively. The certified reference material (SLRS-5 (Fornieles et al. 2011; Rueda-Holgado et al. 2012)) was used for accuracy testing. Anions were measured by ion chromatography (Dionex, ICS-90, Sunnyvale, CA, USA). Total and ferric Fe in water was measured by a spectrophotometric method (UV-9000s, METASH, Shanghai, China) with 1,10-phenanthroline at 510 nm as described previously (Rice et al. 2012; Tamura et al. 1974).

Geochemical parameters in the sediments

Sediment samples were freeze-dried by vacuum freeze-drying equipment (FD-1A-80, Beijing, China) and thoroughly ground using a mortar and pestle before passing through a 200-mesh sieve. To measure anions in sediments, 2 g of dry sediment was mixed with 10 mL of Milli-Q water, shaken for 5 min, and left to equilibrate for 4 h. The supernatant was then centrifuged at 3500×*g* for 15 min and filtered through a 0.45-μm filter membrane. The filtered sample was then used for the determination of anions using ion chromatography (DIONEX ICS-1500, Sunnyvale, USA). Total sulfur (TS), soluble sulfur, total hydrogen (TH), total carbon (TC), and total organic carbon (TOC) in the sediments were measured by an elemental analyzer (Elementar, Hanau, Germany) (Schumacher 2002). The sediment samples were fully digested with HNO_3 and HF (5:1, *v*/*v*) (Edgell 1989), and the major and trace elements were determined by ICP-OES (Vista MPX, Varian, USA) and ICP-MS (Agilent, 7700x, CA, USA), respectively. The certified reference materials (SLRS-5) and internal standards (Rh) were used for accuracy testing. The standard reference material GBW07310 (Chinese National Standard) was used for analytical quality control (Sun et al. 2016). Three measurements of a single sample were performed for each geochemical parameter.

SEM and EDX

Scanning electron microscopy (SEM) analysis was used to determine the presence and morphology of minerals in the sediments based on a protocol described previously (McBeth et al. 2013). SEM images were taken on a field-emission scanning electron microscope (JSM-6460LV, JEOL, Tokyo, Japan) with an EDAX energy-dispersive X-ray spectrometer (EDAX-GENESIS, Mahwah, USA). The SEM was operated at 15 kV with a working distance of 10 mm. For X-ray analysis, an accelerating voltage of 20 kV was used to obtain sufficient X-ray counts.

Sequential extraction of Fe minerals

A sequential Fe extraction procedure (Oni et al. 2015; Poulton and Canfield 2005) was performed to detect the Fe adsorbed to particle surfaces as well as bound in carbonates and Fe oxides. The leaching agents and reaction time are summarized in Table S1. Fe-extractable fractions were measured by a spectrophotometric method (UV-9000s, Shanghai METASH) with 1,10-phenanthroline at 510 nm (Tamura et al. 1974).

Illumina sequencing of 16S rRNA genes and the pipeline for sequence analysis

Total genomic DNA was extracted from 5 g of homogenized sediment samples using the FastDNA® spin kit (MP bio, Santa Ana, USA) following the manufacturer's protocol. All DNA extracts were stored at −80 °C until further analysis. DNA concentration and purity were monitored on 1 % agarose gels. The V4–V5 region of 16S rRNA gene was amplified using the 515f/907r primer set (515f:5′-GTGYCAGCMGCCGCGGTAA-3′, 907r:5′-CCYCAATTCMTTTRAGTTT-3′) (Ren et al. 2014). The merged reads were then assigned to samples based on the barcodes and trimmed by removing the barcode and primer sequences. The raw reads were filtered using split_libraries_fastq.py in QIIME (V1.7.0) with the following criteria: maximum number of consecutive low-quality base calls = 3, minimum number of consecutive high-quality base calls as a fraction of the read length = 0.75, and no base calls

with Phred score <3 (Bokulich et al. 2013; Caporaso et al. 2010). The tags were then compared with the Gold reference database (http://drive5.com/uchime/uchime_download.html) using UCHIME (http://www.drive5.com/usearch/manual/uchime_algo.html) to detect and remove chimeric sequences (Haas et al. 2011). UPARSE was used to cluster operational taxonomic units (OTUs) at 97 % similarity, and the RDP classifier (Version 2.2, http://sourceforge.net/projects/rdp-classifier/) was used to assign taxonomy (DeSantis et al. 2006; Wang et al. 2007) based on the Green Genes Database (http://greengenes.lbl.gov/cgi-bin/nph-index.cgi). Alpha diversity indices were used to estimate species richness for the 12 libraries (Schloss et al. 2009). The reads were deposited into the NCBI Short Read Archive database under accession number of SRP072800.

Data analyses

The similarity of microbial communities among different sediment samples was determined using UniFrac analysis. QIIME calculates both weighted and unweighted UniFrac. Principal coordinate analysis (PCoA) and unweighted pair group method with arithmetic mean (UPGMA) clustering were conducted by unweighted and weighted UniFrac based on the protocol published previously (Kuczynski et al. 2012). Linear discriminant analysis (LDA) effect size (LEfSe) (http://huttenhower.sph.harvard.edu/lefse/) was used to characterize features differentiating the microbial communities under different conditions as described previously (Ling et al. 2014; Segata et al. 2011). LEfSe uses the Kruskal-Wallis rank sum test to detect features with significantly different abundances of assigned taxa and performs LDA to estimate the effect size of each feature with a normalized relative abundance matrix. All tests for significance were two-sided, and p values <0.05 were considered statistically significant. In the current study, two separate LEfSe analyses were performed with samples grouped either by location in the watershed (upstream sediment vs. downstream sediment) or by distinct habitats (AU sediment, AMD creek mat, or contaminated soil). Canonical correspondence analysis (CCA) performed by CANOCO 4.5 (Microcomputer Power, Ithaca, NY, USA) was used to identify chemical properties that structured the microbial community. CCA was done on abundant bacterial genera (i.e., relative abundance >1 % in at least one sequencing library) and selected environmental parameters (TOC and Fe-extractable fractions). Manual forward selection with Monte Carlo permutation was then performed to determine the significance of the environmental variables with 999 permutations (Lepš and Šmilauer 2003). The correlations between TOC and the dominant phyla and genera and diversity indices were determined by Spearman's rank correlation using SPSS (v19, IBM, Armonk, USA).

Results

Environmental parameters in the AMD creek

The water samples collected from the seven sampling sites are characterized by remarkably low pH (2.5–2.7) and elevated total soluble Fe and Fe(III) (Table S2). Total soluble Fe ranged from 675.4 ± 5.4 mg/L in the mine adit to more than 800 mg/L downstream. Aqueous Fe(III) at the mine adit was 265.8 ± 2.1 mg/L, gradually increasing to more than 400 mg/L downstream. It is notable that concentrations of soluble Fe(III) in the cascade AU decreased slightly along the flow path, ranging from 491.5 ± 4.0 mg/L in AU1 to 450.7 ± 5.8 mg/L in AU4. This suggests some precipitation of Fe(III) in the AUs. The whole creek demonstrated elevated aqueous SO_4^{2-} concentrations (>6000 mg/L). In contrast, NO_3^- concentrations were less than 10 mg/L along the creek. Other metallic elements including K, Na, Ca, Mg, and Mn were measured in the water samples as well (Table S3). The mine waters contained less K, Na, and Mn in comparison to Ca and Mg. It is worth noting that concentrations of these major elements did not change substantially along the AMD flow.

The sediments, mats, and soils were also acidic with pH less than 3 in 12 samples (Table S4). Eh was greater than +400 mV in all samples except CS02 (187 mV), suggesting that oxidized environments prevail in both the water and sediments. Like the water samples, the sediments also demonstrated elevated SO_4^{2-} concentrations, ranging from 1565 ± 132.9 to 6425 ± 124.1 mg/kg. Elevated total sulfur (TS) was observed along the watershed, ranging from 4.78 ± 0.41 to 9.06 ± 0.45 %. Sediment and soil samples could be regarded as low-C samples: Most samples had total carbon (TC) and total organic carbon (TOC) percentages less than 3 %, but two samples from the mine adit had relatively higher TOC percentages (5.42 ± 0.11 to 8.62 ± 1.92 %). The creek and adjacent areas demonstrated low total N content (<0.5 % in all samples), indicating a low-N input from the AMD. These sediment samples contained more Mg, Na, and Ca than Mn. More specially, Mg and Ca were accumulated in the AUs, while K demonstrated higher concentrations in the mine adit (Table S5).

Sequential Fe extraction

The procedure for four Fe-extractable fractions is described in Table S1 and measured in the sediment, mat, and soil samples (Table 1). All samples demonstrated high total Fe concentrations (Fetot), ranging from 148.2 ± 6 mg/g upstream to 437.6 ± 5.9 mg/g in midstream due to precipitation from the mine water. Fetot then decreased slightly in downstream sediment samples. The concentrations of four Fe-extractable

Table 1 Fe sequential extractable speciation in sediment samples ((mean ± standard deviation of 3 measurements in mg/g)

Sample	Fetot	FeCarb	FeOX1	FeOX2	FeMag
HX01	290.2 ± 17.8	50.8 ± 0.4	79.6 ± 0.1	36.9 ± 0.1	56.8 ± 0.1
HX02	148.2 ± 6	19.5 ± 0.1	9.5 ± 0.9	7.4 ± 0.1	23.4 ± 0.6
HX03	431.8 ± 6.1	35.5 ± 0.4	138.3 ± 0.4	24.9 ± 0.1	50.6 ± 0.3
HX04	276.9 ± 6	69.9 ± 0.1	9.2 ± 0.1	13.4 ± 0.2	63.7 ± 0.1
AU01	412.9 ± 5.8	26.2 ± 0.1	139.9 ± 0.1	20.0 ± 0.1	70.1 ± 0.6
AU02	243.8 ± 0.6	46.0 ± 0.5	93.6 ± 0	14.9 ± 0.1	39.3 ± 0.2
AU03	302.4 ± 0.9	15.2 ± 0.2	171.8 ± 0.1	11.8 ± 0.9	48.3 ± 0.4
AU04	437.6 ± 5.9	31.4 ± 0.1	147.4 ± 0.1	23.2 ± 0.1	84.8 ± 0.4
CS01	376.4 ± 5.9	22.1 ± 0.1	151.4 ± 0.2	19.2 ± 0.1	57.0 ± 0.1
CS02	437.0 ± 0.8	38.1 ± 0.5	140.2 ± 0.5	28.4 ± 0.7	74.7 ± 0.8
CS03	431.4 ± 0.9	21.2 ± 0.1	156.6 ± 0.3	30.0 ± 0.7	124.9 ± 0.3
CS04	362.9 ± 0.8	40.1 ± 0.2	83.5 ± 0.5	7.4 ± 0.2	89.7 ± 0.2

Fetot total Fe concentration, *FeCarb* adsorbed Fe and Fe carbonates, *FeOX1* amorphous or polycrystalline Fe(oxyhydr)oxides, *FeOX2* crystalline Fe (oxyhydr)oxides, *FeMag* crystalline Fe (oxyhydr)oxides

fractions did not demonstrate a clear site-specific pattern. Among the four Fe-extractable fractions, FeOX1, referring to amorphous and crystalline Fe (mainly ferrihydrite and lepidocrocite) (Oni et al. 2015), was most abundant. FeOX1 exhibited relatively high concentrations (>80 mg/g) in ten samples, but lower in HX01 (9.5 ± 0.9 mg/g) and HX04 (9.2 ± 0.1 mg/g). These two samples were located in mine adit (HX01) and downstream (HX04). In comparison, FeOX2 (crystalline Fe(oxyhydr)oxides, mainly goethite and hematite) and FeMag (crystalline Fe(oxyhydr)oxides, mainly magnetite and maghemite) (Oni et al. 2015) accounted for smaller portion of Fetot. FeCarb containing adsorbed Fe and Fe carbonates was most abundant in HX04 (69.9 ± 0.1 mg/g, downstream), HX01 (50.8 ± 0.4 mg/g, mine adit), and CS04 (40.1 ± 0.2 mg/g, contaminated soil) but was relatively lower in other samples. SEM-energy-dispersive X-ray spectrometer (EDX) demonstrated the co-occurrence of high Fe and O peaks, providing additional evidence for the presence of Fe(oxyhydr)oxides in the tested samples (Fig. S1).

Analysis of Illumina-derived dataset

In total, Illumina sequencing resulted in 691,948 sequencing reads after quality filtering, ranging from 52,294 to 69,661 reads per sample, and clustered into 1475 operational taxonomic units (OTUs). OTU (97 % sequence similarity) numbers ranged from 212 to 677 per sample. The greatest numbers of OTUs were found in the mine adit sediment samples, HX01 (668) and HX02 (651), and sediment in AU (AU04, 677), while the lowest numbers were found in contaminated soils, CS02 (293) and CS03 (212). Other alpha diversity indexes such as Shannon index and Chao 1 index demonstrated the very similar trend as OTU numbers (Table S6).

Taxonomic composition of microbial communities

A total of 33 phyla were identified from the 12 sediments and soil samples (Fig. 2). Among them, *Proteobacteria* predominated in all samples, constituting up to 71.9 % of total bacterial reads (12.8 to 95.3 % per sample). It is notable that *Proteobacteria* was more abundant in AU sediments and contaminated soils, while it accounted for smaller fraction in the AMD creek mats adjacent to the mine adit (HX01, HX02, and HX03, 12.7 to 44.4 %). *Firmicutes* (11.3 % of total reads) and *Actinobacteria* (8.6 % of total reads) ranked as the second and third most abundant phyla, respectively. These two phyla were more abundant in three samples adjacent to the mine adit (HX01, HX02, and HX03) and less abundant in other samples. The remaining 30 phyla accounted for only 8.2 % of total reads. At the class level, *Gammaproteobacteria* was the most abundant class, followed by *Bacilli*, *Acidimicrobiia*, and *Alphaproteobacteria*. *Gammaproteobacteria* was dominant in the sediment of AUs, contaminated soils, and downstream creek mats (Fig. S2), accounting for more than 80 % relative abundance in all these samples except for AU04 (59.4 %). *Bacilli* and *Acidimicrobiia* were more abundant in the upstream creek sediments.

The spatial resolution of microbial taxa was more apparent at the genus level: Microbial communities from the three upstream sediments were very different from those in the downstream samples (Fig. 3). Two OTUs, affiliated with the phyla TM6 and *Firmicutes* (family and genus unclassified), were dominant in the mine adit but undetected in many downstream samples. *Alicyclobacillus* was dominant in the upstream samples but much less abundant in the downstream counterparts. Other genera showing higher abundances in upstream samples included *Iamia*,

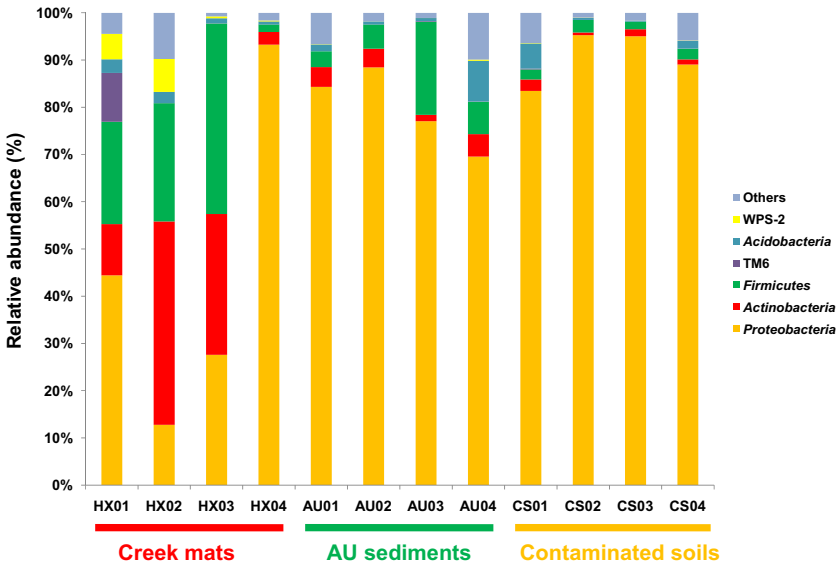

Fig. 2 Major taxonomic groups of bacterial reads retrieved from sediment samples at phylum level

Acidithrix, *Thermogymnomonas*, *Acidiphilium*, and *Metallibacterium*. Two genera (*Halomonas* and *Shewanella*) were dominant in downstream samples. *Halomonas* accounted for more than 40 % of relative abundances in many downstream samples. A Cytoscape network demonstrated the difference of major genera between upstream and downstream samples (Fig. S3).

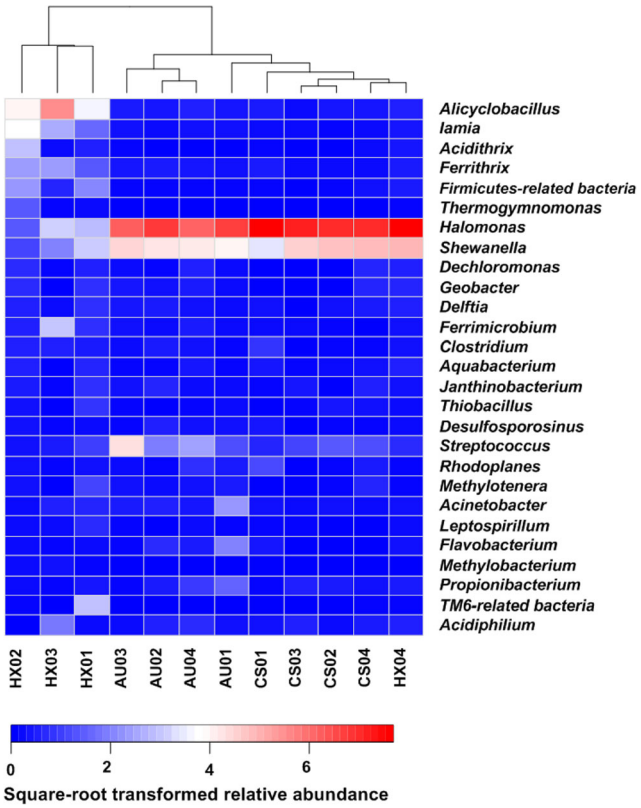

Fig. 3 Heatmap of the distribution of abundant genera with relative abundances >1 % in at least one sample. Double hierarchical dendrogram showed the microbial distribution of the six samples. The root-square-transformed relative percentage values for the microbial genera are indicated by *hue*

Comparison of bacterial communities between different zones

Cluster analysis including weighted UPGMA tree and PCoA was used to better elucidate the differences among microbial communities. Roughly, microbial communities can be divided into two groups according to the UPGMA tree (Fig. S4). Group I includes samples from upstream AMD creek sediments including HX01, HX02, and HX03. Group II included the rest of the samples and could be further divided into two subgroups containing AU04 and AU03 (sediments samples from AU) versus all other samples in this group. CS03 (contaminated soil) and HX04 (mat samples from downstream creek) were more closely related to each other than other samples. PCoA revealed that downstream mats and contaminated soils clustered together, while the three upstream samples were more distant from the other samples (Fig. 4). In addition to the grouping dividing samples according to their habitats (i.e., soils, sediments, and mats), a second grouping based on microbial community similarity (upstream samples versus downstream samples) was revealed by the cluster analysis.

In order to find specialized bacterial groups enriched within each type of sediments, we performed the LEfSe from phylum to genus level (Segata et al. 2011) according to two different grouping patterns. In the first LEfSe analysis (LEfSe A) (Fig. 5), microbial populations were grouped as upstream sediment samples including HX01, HX02, and HX03 and downstream sediment samples including the rest. In the second LEfSe analysis (LEfSe B) (Fig. S5), microbial populations were divided into three groups as creek mat (creek), sediment of AU (built), and contaminated soils (terre). Cladograms

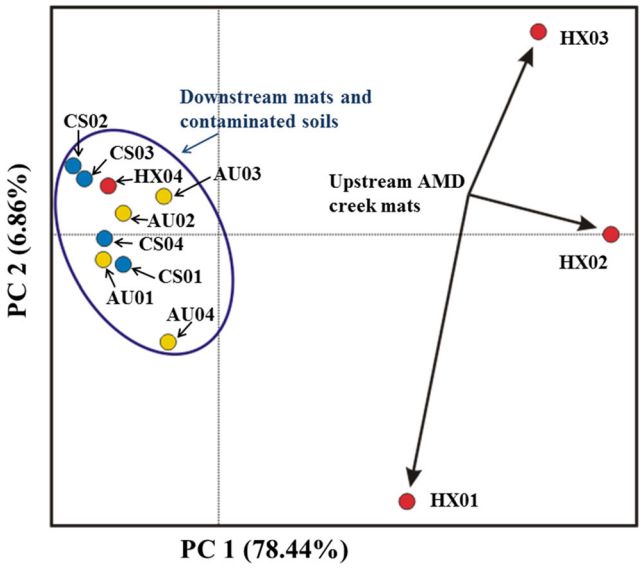

Fig. 4 The PCoA plot showing clusters of microbial communities based on weighted UniFrac with 100 % support at all nodes (*bottom*: the percentages are the percentage of variation explained by the components

showed taxa with LDA values higher than 3.6 for clarity. In LEfSe A, there were five taxonomic groups from phylum to family enriched in the upstream samples, namely, *Firmicutes* (phylum) to *Alicyclobacillaceae* (family), *Actinobacteria* (phylum) to *Acidimicrobiaceae* (family), *Xanthomonadales* (order) to *Xanthomonadaceae* (family), *Rhodobiaceae* (family), and *Afifella* (genus). The bacterial lineages enriched in the downstream samples were from *Proteobacteria* (phylum) to *Shewanella* (genus), and *Streptococcaceae* (family) to *Streptococcus* (genus). In contrast, LEfSeB did not reveal significant variations in bacterial taxa among three groups. Only *Acidimicrobiales* (subclass), *Acidimicrobiia* (class), and *Acidimicrobiaceae* (order) within the phylum *Actinobacteria* showed an LDA value greater than 4 in the AMD creek mat samples. In the soils, *Rhizobiales* (order) to *Methylobacteriaceae* (family) was the only taxa enriched (LDA >4). Two bacterial lineages from *Lactobacillales* (order) and *Streptococcaceae* (family) were enriched in AUs (LDA >4).

Effects of environmental parameters on microbial community composition

CCA was conducted to discern the possible correlations between environmental variables and bacterial community structure, as represented by the major taxonomic groups (genera) (Fig. 6). Axis 1 explained 54.1 % of the genus-level variability and was positively correlated with TOC and FeOX2 and negatively correlated with SO_4^{2-} and the rest of Fe-extractable fractions. Axis 2 explained a further 17 % of the variability and was positively correlated with all tested parameters except TOC. As indicated by the length of the environmental variables arrows in the CCA biplot, the strongest determinant for the overall microbial communities was TOC. TOC was positively correlated with two upstream samples, HX01 and HX02, but was negatively correlated with most downstream samples. The relative magnitudes of the vectors associated with Fe indicate that FeMag is not as strongly correlated to the community composition as Fetot, FeCarb, and FeOX1.

Discussion

This AMD-contaminated site, Huaxi creek and adjacent contaminated soil, harbored a wide diversity of microorganisms known to thrive in acidic environments, providing an excellent field-based site to study microbial Fe and S cycling under this extreme habitat. Based on UPGMA tree and PCoA analyses, microbial communities in the upstream sediments differed from those in the downstream samples. We found higher diversity in the upstream sediments compared to the downstream samples. These patterns were manifested at all phylogenetic levels but were most apparent at the genus level. Our observation of decreasing diversity from upstream to downstream is similar to the decrease in diversity from headwater to river mouth described in several large river networks (Crump et al. 2012; Savio et al. 2015). Crump et al. suggest that such patterns of diversity are structured by initial inoculation from soils followed by a species-sorting process (i.e., the selection by local environmental conditions) during downslope dispersal of both common and rare microorganisms (Crump et al. 2012). We proposed that the mining area acts as the initial inoculum of microorganisms to the small watershed. In addition, similar to the previously published studies identifying persistent and ubiquitous core communities along river stretch (Savio et al. 2015; Staley et al. 2013), such core microbial consortia were also identified in most downstream samples in the present study. The main phylotypes of the core communities, including *Halomonas* and *Shewanella* spp., reflect their competence in such harsh environments.

This clear spatial pattern of bacterial community composition is attributed to the remarkable contrast in environmental conditions. One of the notable findings was that TOC content may be the primary environmental parameter in structuring the differences in microbial communities between upstream and downstream samples. Based upon CCA, TOC demonstrated the strongest effect on the microbial communities. Microbial communities from three upstream samples were positively correlated with TOC, while the downstream counterparts were negatively correlated with TOC (Fig. 6). We propose that the high TOC content in upstream samples favors the growth of various heterotrophic bacteria, especially heterotrophic FeOB. The composition of TOC may change along the creek and thus results in the remarkable shift in the assemblage of microorganisms. For instance, the TOC in the mine

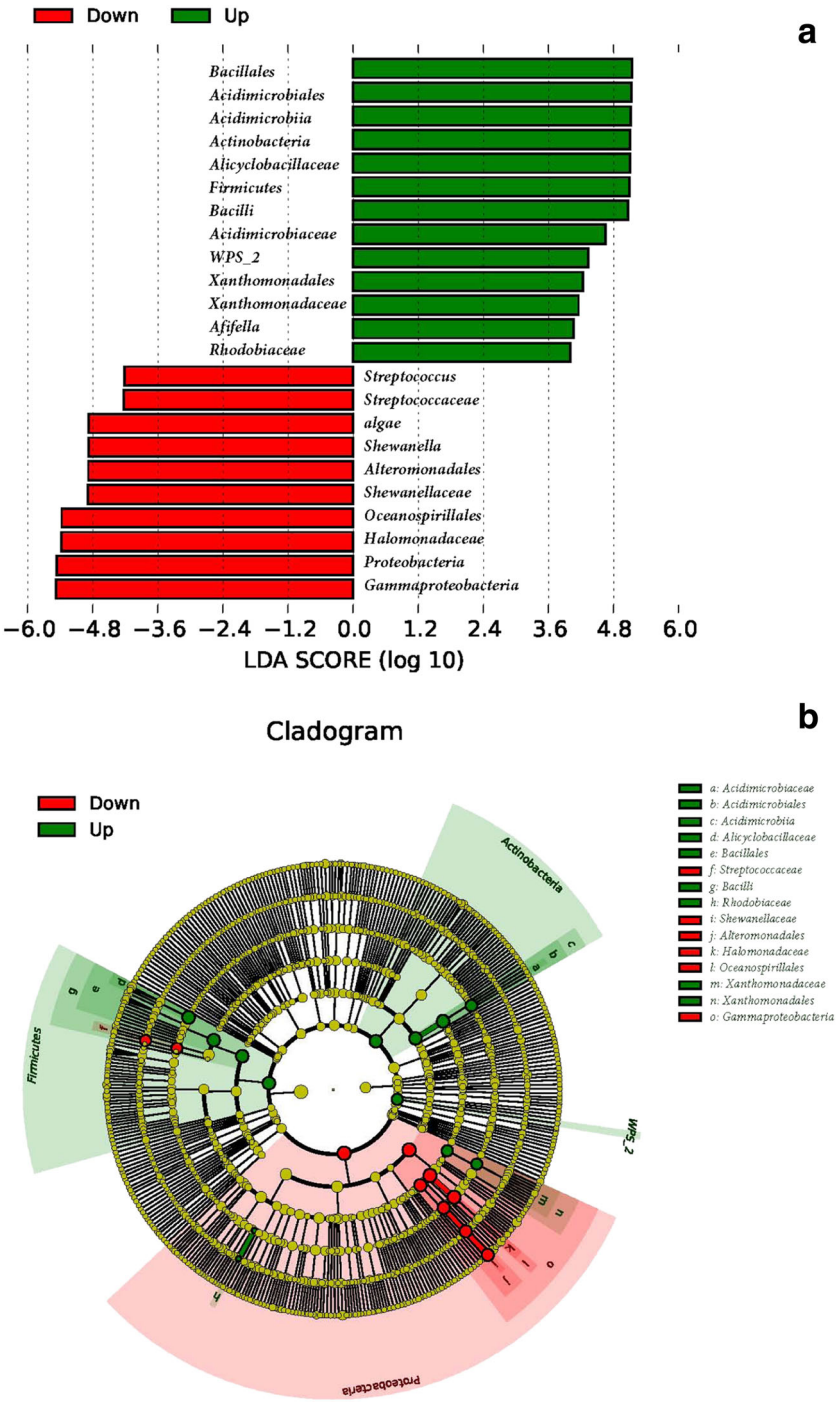

Fig. 5 LEfSe identified the most differentially abundant taxa between upstream sediments and downstream sediments. Taxa enriched in upstream sediments with a positive LDA score (*green*), and taxa enriched in downstream sediments have a negative score (*red*). **a** Only taxa meeting an LDA significance threshold of 3.6 are shown. **b** Taxonomic cladogram obtained from LEfSe analysis of 16S sequences (relative abundance >0.5 % in at least one sample). *Small circles* and *shading* with *different colors* in the diagram represent abundance of those taxa in the respective group. *Yellow circles* represent non-significant differences in abundance between upstream and downstream sediments of those particular taxa. The *brightness* of each *dot* is proportional to its effect size (Color figure online)

adit may originate from the mine water and decaying plant litter (the mine adit is covered by trees), composed of mostly lignin, cellulose, and a number of other organic substrates that could sustain more diverse microbial communities. In comparison, the downstream samples may receive more refractory organic substrates from upstream as reported previously (Savio et al. 2015), which leads to decreasing diversity indices (e.g., Shannon, Chao1, and Simpson) in downstream samples containing the more competitive bacteria along the creek. Our hypothesis was confirmed by Spearman's rank correlation, which indicated that TOC is positively correlated with bacteria diversity such as Shannon and Chao1 (Table S7). In addition to the impact on the overall microbial diversity, TOC was also positively correlated with a number of individual bacterial groups such as *Actinobacteria*, WPS-2, *Alicyclobacillus*, *Iamia*, *Acidithrix*, and TM6-related bacteria (Table S7). The importance of TOC in AMD environments may have environmental implications for future AMD bioremediation.

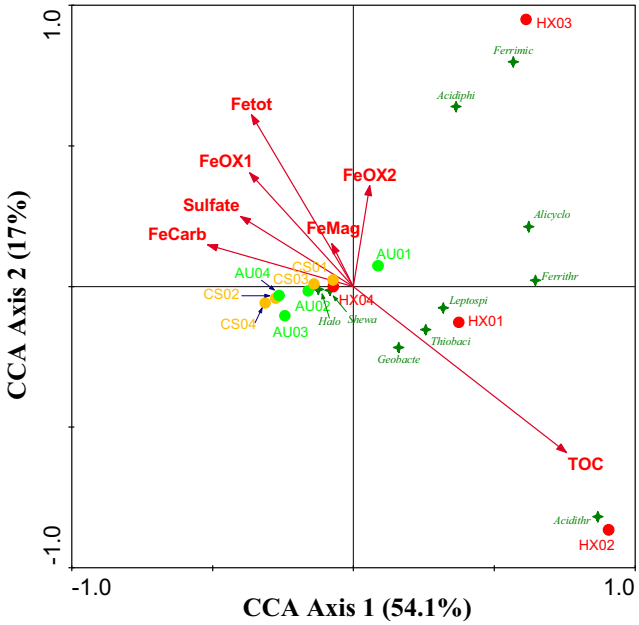

Fig. 6 Ordination diagrams from canonical correspondence analysis (CCA) of bacterial abundances and geochemical parameters. *Colorful circles* indicated the microbial communities (*red*: creek mats; *green*: AU sediments; *orange*: contaminated soil). *Red arrows* indicate the direction and magnitude of geochemical parameters associated with bacterial community structures. *Green stars* indicated the individual genera. A symbol's position in relation to a vector head indicates the correlation between the community and the environmental factors. The length of a vector reflects the relative importance of those environmental factors in discriminating the overall microbial community within one library (Zhang et al. 2008). Please note that microbial communities from creek mats were shown as *red dots*, aeration units were shown as *green dots*, and contaminated soils were shown as *orange dots*. Bacteria abbreviations: *Halo Halomonas*, *Shewa Shewanella*, *Alicyclo Alicyclobacillus*, *Acidiphi Acidiphilium*, *Ferrimic Ferrimicrobium*, *Ferrithr Ferrithrix*, *Leptospi Leptospirillum*, *Thiobaci Thiobacillus* (Color figure online)

The dominance of various acidophilic FeOB suggests that Fe and pH may be primary environmental factors that control AMD-associated microbial communities. CCA indicated that Fetot, FeCarb, FeOX1, and FeOX2 strongly influence the microbial communities. Evidence for microbial Fe-carbonate formation was detected in Rio Tinto, Spain (Sánchez-Román et al. 2014), which revealed an unexplored pathway for carbonate mineralization under acidic conditions mediated by *Acidiphilium* sp. PM, an Fe-reducing bacterium. In the current study site, FeCarb may be formed partially due to microbial activity. FeOX1 and FeOX2 include crystalline Fe (oxyhydr)oxides, which could serve as electron acceptors for FeRB (Kostka et al. 2002; Roden and Urrutia 1999). This observation may support the influence of FeOX1 and FeOX2 on microbial communities. FeMag demonstrated the smallest effect of any of the measured Fe fractions on microbial communities. FeMag consists mainly of magnetite and maghemite, which may be difficult for microorganisms to reduce (Bishop et al. 2010).

In line with elevated Fe concentrations, the microbial communities in the creek are dominated by a wide diversity of FeOB and FeRB, suggesting dynamic microbial Fe cycling at the site. Previous studies have indicated that FeOB can accelerate Fe(II) oxidation rates twofold to fivefold both in pure cultures (Neubauer et al. 2002) and native groundwater seep communities (Rentz et al. 2007). The oxidized Fe(III) then precipitates from the water, which is a kind of bioremediation (Johnson and Hallberg 2005). In the current study, the distribution of Fe-metabolizing bacteria was location-dependent. FeOB were dominant and very diverse in the upstream sediments (Fig. S3). *Alicyclobacillus* spp., which make up the most common genus in AMD environments (Méndez-García et al. 2015), had relative abundances greater than 10 % in the three upstream samples but were <0.5 % downstream (Fig. 7). *Alicyclobacillus* spp. contain members such as *Alicyclobacillus ferrooxydans*, which is able to oxidize Fe(II) in acidic environments (Jiang et al. 2008), and *Alicyclobacillus aeris*, which was isolated from

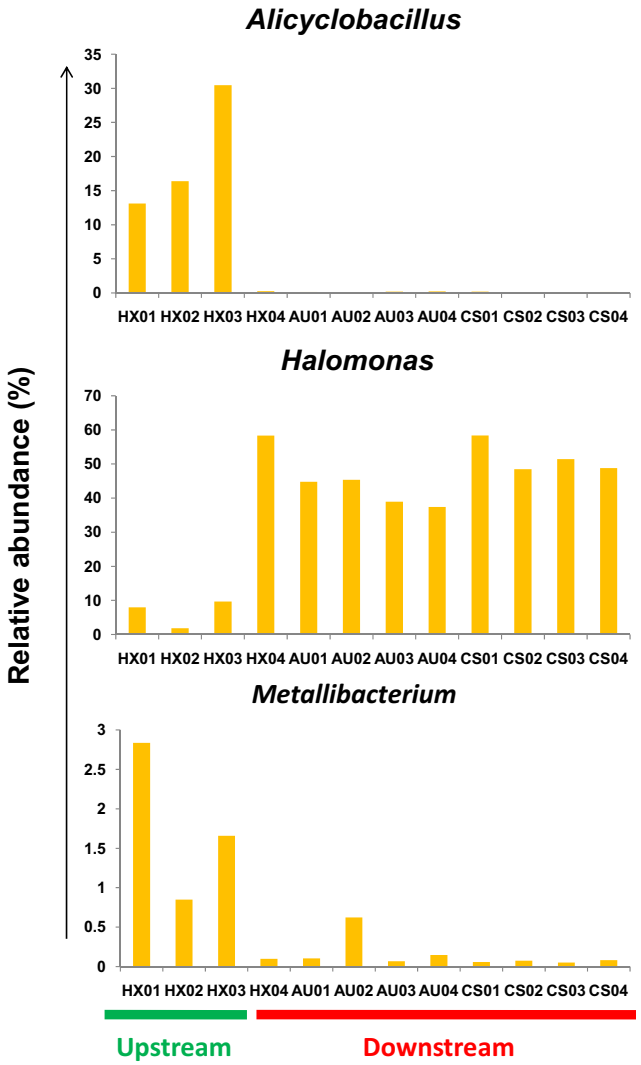

Fig. 7 The relative abundance (%) of dominant Fe(II)-oxidizing bacteria among the upstream and downstream samples

a copper mine and can oxidize both Fe and S (Guo et al. 2009). The *Alicyclobacillus*-related OTU identified in the current study was closely related (97 % sequence similarity of 373 bp) to *Alicyclobacillaceae* bacterium Y002 isolated from acidic sediments (Lu et al. 2010).

Sequences closely related to the genus *Metallibacterium* were also enriched in upstream samples (Fig. 7). These sequences were closely related to uncultured clones isolated from AMD (100 % sequence similarity, accession number: JX297618) (Brofft et al. 2002; Guo et al. 2013; Mendez et al. 2008) and *Metallibacterium scheffleri* (99 % sequence similarity of 374 bp). *M. scheffleri*, isolated from acidic biofilms, is able to oxidize Fe(II) and reduce Fe(III) (Ziegler et al. 2013). A number of potential Fe-metabolizing bacteria clustered within the phylum *Actinobacteria* were also enriched in the upstream samples. Namely, *Ferrithrix* spp. were enriched in three upstream sediments, while *Ferrimicrobium* spp. were only enriched in HX03. Both of these genera contain heterotrophic FeOB (Johnson et al. 2009), suggesting that the high TOC in the upstream samples may be used as carbon and energy sources by these bacteria. The *Ferrithrix*-related OTUs were closely related to *Ferrithrix thermotolerans* (94 % sequence similarity of 377 bp) (Johnson et al. 2009), and the *Ferrimicrobium*-related OTUs were closely related to *Ferrimicrobium* sp. Py-F2 (92 % sequence similarity of 377 bp) (Kay et al. 2013), all of which are extremely acidophilic bacteria.

One potential FeOB, *Halomonas*, predominated (>35 %) in all downstream samples (Fig. 7). *Halomonas* spp. have been identified as Mn(II)-oxidizing bacteria (Homann et al. 2009; Templeton et al. 2005) and were proposed as FeOB as well (Homann et al. 2009). In another study, *Halomonas* spp. have been found in high abundance in hydrothermal fields with high Fe concentrations, suggesting their potential role in Fe cycling (Kaye et al. 2011). *Halomonas* spp. have also been detected in AMD environments (Auld et al. 2013; Santofimia et al. 2013; Sun et al. 2015b). Taken together, we propose that *Halomonas* are the major FeOB in the downstream samples of the current AMD creek.

Compared with FeRB, very few sequences belonging to sulfate-reducing bacteria (SRB) were detected in the current study; even high concentrations of SO_4^{2-} were detected in all the samples. A possible explanation for this observation is that Fe(III) reduction in acidic conditions should be more energetically favorable than sulfate reduction (Emmerich et al. 2012). The redox potential of the Fe(III)/Fe(II) pair is high (+770 mV) at pH 1 in comparison to the equivalent couple at neutral pH (ranging from +100 to −300 mV depending on the form of Fe(III) mineral (Straub et al. 2001)). This makes Fe(III) nearly equivalent to molecular oxygen as an electron acceptor in acidic environments. Given the elevated Fe(III) and high Eh in the creek, FeRB may outcompete sulfate reducers for organic electron donors. Therefore, FeRB constitute a very important bacterial group for AMD bioremediation due to the acidic environments in most AMD environments.

Among the FeRB, *Shewanella* was the most dominant genus, detected in all 12 samples, and accounting for 15.8 % of total reads. *Shewanella* occurred at higher abundances in downstream samples (Fig. 8). It is surprising to see the dominance of *Shewanella* in such extreme acidic environments because *Shewanella* are usually regarded as neutrophilic FeRB and are seldom detected in AMD environments (Ivanova et al. 2003). In previous studies, we detected large numbers of *Shewanella* in the sediments of an AMD-impacted creek and in rice paddy soils irrigated by AMD waters (Sun et al. 2015a, b), suggesting that these bacteria may be able to tolerate to low pH and thrive in acidic Fe-rich environments. *Acidiphilium* contains acidophilic bacteria that are able to reduce Fe(III) (Küsel et al. 1999), such as *Acidiphilium*

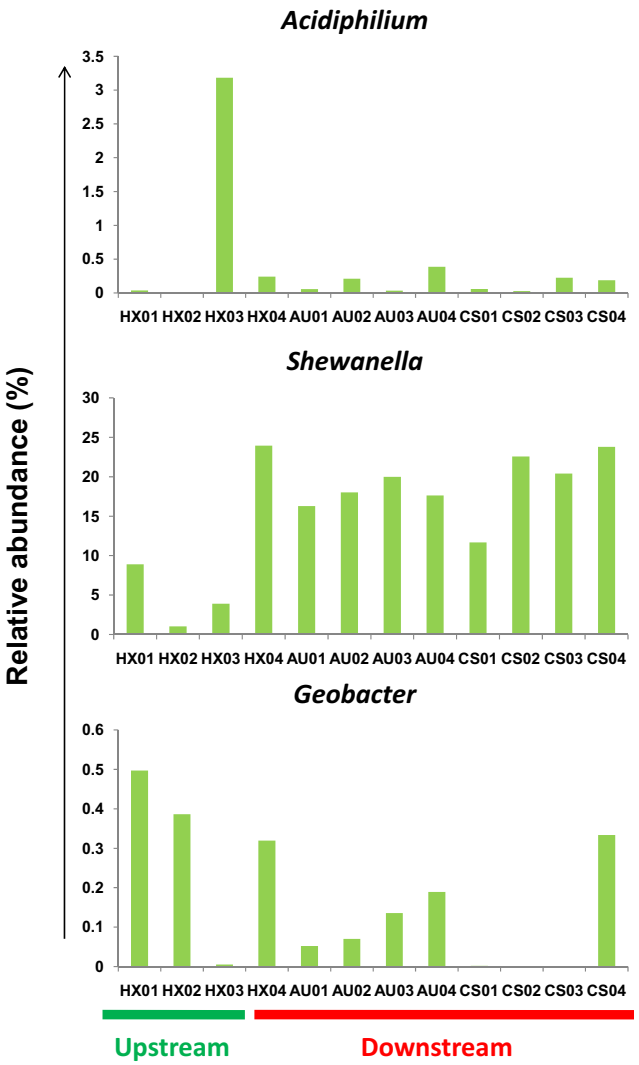

Fig. 8 The relative abundance (%) of dominant Fe(III)-reducing bacteria among the upstream and downstream samples

acidophilum (Liu et al. 2011) and *Acidiphilium cryptum* (Harrison 1981). *Acidiphilium* exhibited relatively high abundance in the mat samples close to mine adit (HX03) and was detected in all samples (Fig. 8). Compared to *Shewanella* and *Acidiphilium*, another notable FeRB, *Geobacter*, was present at low abundance throughout the study area. This may be attributed to the low tolerance of *Geobacter* to acidic environments (Lovley et al. 1993). Acidophilic FeRB such as *Acidocella* and neutrophilic FeRB such as *Geothrix* were also found but were in low abundances in individual samples. The high abundances of both FeOB and FeRB suggest dynamic Fe cycling in the current ecosystem. Such co-occurrence of FeOB and FeRB may have beneficial effect to each group: Heterotrophic FeRB can stimulate growth of autotrophic FeOB both by producing reduced Fe and by removing excess TOC, which can be inhibitory to autotrophic FeOB. In turn, autotrophic FeOB can fix CO_2 to produce organic substrates for FeRB growth (Bacelar-Nicolau and Johnson 1999).

A number of OTUs which could not be placed within any known taxonomic group were highly enriched in the upstream samples. For example, a TM6-related OTU was highly abundant (8.1 %) in the mine adit. Microorganisms belonging to the candidate phylum TM6 have been referred to as the "dark matter of life" as the entire divisions of bacterial phyla that have yet to be cultivated or sequenced (McLean et al. 2013). The TM6-related OTU was closely related to an uncultured bacterial clone collected in deep-sea methane-seep sediment (97 % sequence similarity of 373 bp) (Aoki et al. 2014). A *Firmicutes*-related OTU enriched in the mine adit (HX01 and HX02) was closely related to a number of uncultured clones detected in AMD environments (100 % sequence similarity of 373 bp, accession numbers: KF581285 and GU979551) (Hao et al. 2010; Ling et al. 2013). However, this OTU did not reveal a close match with any known cultivated isolates, highlighting the unknown role of these *Firmicutes*-related OTUs in AMD-associated environments. Unfortunately, we cannot predict the metabolic functions of these OTUs merely based on the phylogenetic information. Pure cultures would be needed to reveal the fully physiological information of these enigmatic taxa.

The low pH and high Fe at the current study site create unique microbial communities dominated by acidophilic FeOB and FeRB. Besides the pH and different Fe fractions, TOC may play an important role in shaping the indigenous microbial communities, especially the acidophilic FeOB. Future studies should address the role of TOC composition changes in controlling functional microorganisms. In comparison to various geochemical parameters, microbial communities were not structured by their habitats. The second LEfSe analysis showed that no matter whether the samples were taken from the creek, soils, or AUs, there were no obvious differences of microbial communities based on this grouping pattern (Fig. S5). We therefore conclude that contemporary factors (in situ geochemical parameters) may be the primary filters in structuring the microbial community, while historical factors (i.e., mats, soils, and sediments) do not exert strong impact on microbial assemblages.

Microbial communities in upstream sediments were characterized with a wide diversity of acidophilic FeOB and FeRB, while downstream sediments were dominated by a single FeOB (*Halomonas*) and a single FeRB (*Shewanella*). The results described here could be generated as a geomicrobiological model (Fig. S6) and provide insights for in situ bioremediation of AMD contamination: By controlling the redox conditions, pH, and TOC contents, one may control the distribution of various functional microbial groups (e.g., FeOB, FeRB, or SRB) and take advantage of such microorganisms for in situ bioremediation. Future studies should address the metabolic pathways and identification of the functional genes, which will help us better understand natural attenuation of AMD in the contaminated sites.

Compliance with ethical standards

Funding This research was funded by the Public Welfare Foundation of the Ministry of Water Resources of China (201501011), the National Natural Science Foundation of China (41103080, 41173028), the Opening Fund of the State Key Laboratory of Environmental Geochemistry (SKLEG2015907), and Guangdong Academy of Sciences (REN [2015] 20). We thank Prof. Margarete Kalin, Dr. Bill Wheeler, and Dr. Carlos Paulo at the Boojum Research Ltd. for technical support.

Conflict of interest The authors declare that they have no conflict of interest.

Ethical approval This article does not contain any studies with human participants performed by any of the authors.

References

Aoki M, Ehara M, Saito Y, Yoshioka H, Miyazaki M, Saito Y, Miyashita A, Kawakami S, Yamaguchi T, Ohashi A (2014) A long-term cultivation of an anaerobic methane-oxidizing microbial community from deep-sea methane-seep sediment using a continuous-flow bioreactor. PLoS One 9:105356–105364

Auld RR, Myre M, Mykytczuk N, Leduc LG, Merritt TJ (2013) Characterization of the microbial acid mine drainage microbial community using culturing and direct sequencing techniques. J Microbiol Methods 93:108–115

Bacelar-Nicolau P, Johnson DB (1999) Leaching of pyrite by acidophilic heterotrophic iron-oxidizing bacteria in pure and mixed cultures. Appl Environ Microbiol 65:585–590

Baker BJ, Banfield JF (2003) Microbial communities in acid mine drainage. FEMS Microbiol Ecol 44:139–152

Bishop ME, Jaisi DP, Dong H, Kukkadapu RK, Ji J (2010) Bioavailability of Fe (III) in loess sediments: an important source of electron acceptors. Clay Clay Miner 58:542–557

Bokulich NA, Subramanian S, Faith JJ, Gevers D, Gordon JI, Knight R, Mills DA, Caporaso JG (2013) Quality-filtering vastly improves diversity estimates from Illumina amplicon sequencing. Nat Methods 10:57–59

Brofft JE, McArthur JV, Shimkets LJ (2002) Recovery of novel bacterial diversity from a forested wetland impacted by reject coal. Environ Microbiol 4:764–769

Caporaso JG, Kuczynski J, Stombaugh J, Bittinger K, Bushman FD, Costello EK, Fierer N, Pena AG, Goodrich JK, Gordon JI (2010) QIIME allows analysis of high-throughput community sequencing data. Nat Methods 7:335–336

Crump BC, Amaral-Zettler LA, Kling GW (2012) Microbial diversity in arctic freshwaters is structured by inoculation of microbes from soils. ISME J 6:1629–1639

Das T, Ayyappan S (1999) Factors affecting bioleaching kinetics of sulfide ores using acidophilic micro-organisms. Biometals 12:1–10

DeSantis TZ, Hugenholtz P, Larsen N, Rojas M, Brodie EL, Keller K, Huber T, Dalevi D, Hu P, Andersen GL (2006) Greengenes, a chimera-checked 16S rRNA gene database and workbench compatible with ARB. Appl Environ Microbiol 72:5069–5072

Edgell K (1989) USEPA method study 37 SW-846 method 3050 acid digestion of sediments, sludges, and soils. US Environmental Protection Agency, Environmental Monitoring Systems Laboratory

Emmerich M, Bhansali A, Losekann-Behrens T, Schroder C, Kappler A, Behrens S (2012) Abundance, distribution, and activity of Fe(II)-oxidizing and Fe(III)-reducing microorganisms in hypersaline sediments of Lake Kasin, Southern Russia. Appl Environ Microbiol 78: 4386–4399

Fornieles AC, de Torres AG, Alonso EV, Cordero MS, Pavón JC (2011) Speciation of antimony (III) and antimony (V) in seawater by flow injection solid phase extraction coupled with online hydride generation inductively coupled plasma mass spectrometry. J Anal At Spectrom 26:1619–1626

Guo X, Yin H, Cong J, Dai Z, Liang Y, Liu X (2013) RubisCO gene clusters found in a metagenome microarray from acid mine drainage. Appl Environ Microbiol 79:2019–2026

Guo X, You X-Y, Liu L-J, Zhang J-Y, Liu S-J, Jiang C-Y (2009) *Alicyclobacillus aeris* sp. nov., a novel ferrous-and sulfur-oxidizing bacterium isolated from a copper mine. Int J Syst Evol Microbiol 59: 2415–2420

Haas BJ, Gevers D, Earl AM, Feldgarden M, Ward DV, Giannoukos G, Ciulla D, Tabbaa D, Highlander SK, Sodergren E (2011) Chimeric 16S rRNA sequence formation and detection in Sanger and 454-pyrosequenced PCR amplicons. Genome Res 21:494–504

Hallberg K (2010) New perspectives in acid mine drainage microbiology. Hydrometallurgy 104:448–453

Hao C, Wang L, Gao Y, Zhang L, Dong H (2010) Microbial diversity in acid mine drainage of Xiang Mountain sulfide mine, Anhui Province, China. Extremophiles 14:465–474

Harrison AP (1981) *Acidiphilium cryptum* gen. nov., sp. nov., heterotrophic bacterium from acidic mineral environments. Int J Syst Bacteriol 31:327–332

Homann VV, Sandy M, Tincu JA, Templeton AS, Tebo BM, Butler A (2009) Loihichelins A−F, a suite of amphiphilic siderophores produced by the marine bacterium *Halomonas LOB-5*. J Nat Prod 72: 884–888

Ivanova EP, Sawabe T, Hayashi K, Gorshkova NM, Zhukova NV, Nedashkovskaya OI, Mikhailov VV, Nicolau DV, Christen R (2003) *Shewanella fidelis sp. nov.*, isolated from sediments and sea water. Int J Syst Evol Microbiol 53:577–582

Jiang C-Y, Liu Y, Liu Y-Y, You X-Y, Guo X, Liu S-J (2008) *Alicyclobacillus ferrooxydans* sp. nov., a ferrous-oxidizing bacterium from solfataric soil. Int J Syst Evol Microbiol 58:2898–2903

Johnson DB (1995) Acidophilic microbial communities: candidates for bioremediation of acidic mine effluents. Int Biodeterior Biodegrad 35:41–58

Johnson DB (2003) Chemical and microbiological characteristics of mineral spoils and drainage waters at abandoned coal and metal mines. Water Air Soil Pollut 3:47–66

Johnson DB, Bacelar-Nicolau P, Okibe N, Thomas A, Hallberg KB (2009) *Ferrimicrobium acidiphilum* gen. nov., sp. nov. and *Ferrithrix thermotolerans* gen. nov., sp. nov.: heterotrophic, iron-oxidizing, extremely acidophilic actinobacteria. Int J Syst Evol Microbiol 59:1082–1089

Johnson DB, Hallberg KB (2003) The microbiology of acidic mine waters. Res Microbiol 154:466–473

Johnson DB, Hallberg KB (2005) Acid mine drainage remediation options: a review. Sci Total Environ 338:3–14

Küsel K, Dorsch T, Acker G, Stackebrandt E (1999) Microbial reduction of Fe (III) in acidic sediments: isolation of *Acidiphilium cryptum* JF-5 capable of coupling the reduction of Fe (III) to the oxidation of glucose. Appl Environ Microbiol 65:3633–3640

Kay CM, Rowe OF, Rocchetti L, Coupland K, Hallberg KB, Johnson DB (2013) Evolution of microbial "streamer" growths in an acidic, metal-contaminated stream draining an abandoned underground copper mine. Life 3:189–210

Kaye JZ, Sylvan JB, Edwards KJ, Baross JA (2011) *Halomonas* and *Marinobacter* ecotypes from hydrothermal vent, subseafloor and deep-sea environments. FEMS Microbiol Ecol 75:123–133

Kostka JE, Dalton DD, Skelton H, Dollhopf S, Stucki JW (2002) Growth of iron (III)-reducing bacteria on clay minerals as the sole electron acceptor and comparison of growth yields on a variety of oxidized iron forms. Appl Environ Microbiol 68:6256–6262

Kuczynski J, Stombaugh J, Walters WA, González A, Caporaso JG, Knight R (2012) Using QIIME to analyze 16S rRNA gene sequences from microbial communities. Curr Protoc Microbiol 10: 1–20

Lepš J, Šmilauer P (2003) Multivariate analysis of ecological data using CANOCO. Cambridge University Press, Cambridge

Ling Z, Liu X, Jia X, Cheng Y, Luo Y, Yuan L, Wang Y, Zhao C, Guo S, Li L (2014) Impacts of infection with different toxigenic *Clostridium difficile* strains on faecal microbiota in children. Sci Rep 4:7485–7485

Ling Z, Liu X, Luo Y, Yuan L, Nelson KE, Wang Y, Xiang C, Li L (2013) Pyrosequencing analysis of the human microbiota of healthy Chinese undergraduates. BMC Genomics 14:63–70

Liu H, Yin H, Dai Y, Dai Z, Liu Y, Li Q, Jiang H, Liu X (2011) The co-culture of *Acidithiobacillus ferrooxidans* and *Acidiphilium acidophilum* enhances the growth, iron oxidation, and CO2 fixation. Arch Microbiol 193:857–866

Lovley DR, Giovannoni SJ, White DC, Champine JE, Phillips E, Gorby YA, Goodwin S (1993) *Geobacter metallireducens* gen. nov. sp. nov., a microorganism capable of coupling the complete oxidation of organic compounds to the reduction of iron and other metals. Arch Microbiol 159:336–344

Lu S, Gischkat S, Reiche M, Akob DM, Hallberg KB, Küsel K (2010) Ecophysiology of Fe-cycling bacteria in acidic sediments. Appl Environ Microbiol 76:8174–8183

Méndez-García C, Peláez AI, Mesa V, Sánchez J, Golyshina OV, Ferrer M (2015) Microbial diversity and metabolic networks in acid mine drainage habitats. Front Microbiol 6:475. doi:10.3389/fmicb.2015.00475

McBeth JM, Fleming EJ, Emerson D (2013) The transition from freshwater to marine iron oxidizing bacterial lineages along a salinity gradient on the Sheepscot River, Maine, USA. Env Microbiol Rep 5:453–463

McLean JS, Lombardo M-J, Badger JH, Edlund A, Novotny M, Yee-Greenbaum J, Vyahhi N, Hall AP, Yang Y, Dupont CL (2013) Candidate phylum TM6 genome recovered from a hospital sink biofilm provides genomic insights into this uncultivated phylum. Proc Natl Acad Sci U S A 110:2390–2399

Mendez MO, Neilson JW, Maier RM (2008) Characterization of a bacterial community in an abandoned semiarid lead-zinc mine tailing site. Appl Environ Microbiol 74:3899–3907

Neubauer SC, Emerson D, Megonigal JP (2002) Life at the energetic edge: kinetics of circumneutral iron oxidation by lithotrophic iron-oxidizing bacteria isolated from the wetland-plant rhizosphere. Appl Environ Microbiol 68:3988–3995

Oni O, Miyatake T, Kasten S, Richter-Heitmann T, Fischer D, Wagenknecht L, Kulkarni A, Blumers M, Shylin SI, Ksenofontov V (2015) Distinct microbial populations are tightly linked to the profile of dissolved iron in the methanic sediments of the Helgoland mud area, North Sea. Front Microbiol 6:365. doi:10.3389/fmicb.2015.00365

Poulton SW, Canfield DE (2005) Development of a sequential extraction procedure for iron: implications for iron partitioning in continentally derived particulates. Chem Geol 214:209–221

Ren G, Zhang H, Lin X, Zhu J, Jia Z (2014) Response of phyllosphere bacterial communities to elevated CO_2 during rice growing season. Appl Microbiol Biotechnol 98:9459–9471

Rentz JA, Kraiya C, Luther GW, Emerson D (2007) Control of ferrous iron oxidation within circumneutral microbial iron mats by cellular activity and autocatalysis. Environ Sci Technol 41:6084–6089

Rice E, Baird R, Eaton A, Clesceri L (2012) Standard methods for the examination of water & wastewater 22nd edition. American Public Health Association, American Water Works Association, Water Environment Federatio, Washington, DC

Roden EE, Urrutia MM (1999) Ferrous iron removal promotes microbial reduction of crystalline iron (III) oxides. Environ Sci Technol 33:1847–1853

Rojas-Chapana JA, Tributsch H (2004) Interfacial activity and leaching patterns of *Leptospirillum ferrooxidans* on pyrite. FEMS Microbiol Ecol 47:19–29

Rojas J, Giersig M, Tributsch H (1995) Sulfur colloids as temporary energy reservoirs for *Thiobacillus ferrooxidans* during pyrite oxidation. Arch Microbiol 163:352–356

Rueda-Holgado F, Bernalte E, Palomo-Marin M, Calvo-Blazquez L, Cereceda-Balic F, Pinilla-Gil E (2012) Miniaturized voltammetric stripping on screen printed gold electrodes for field determination of copper in atmospheric deposition. Talanta 101:435–439

Sánchez-Román M, Fernández-Remolar D, Amils R, Sánchez-Navas A, Schmid T, San M-UP, Rodríguez N, Mckenzie JA, Vasconcelos C (2014) Microbial mediated formation of Fe-carbonate minerals under extreme acidic conditions. Sci Rep 4:4767–4767

Santofimia E, González-Toril E, López-Pamo E, Gomariz M, Amils R, Aguilera Á (2013) Microbial diversity and its relationship to physicochemical characteristics of the water in two extreme acidic pit lakes from the Iberian Pyrite Belt (SW Spain). PLoS One 8:51–82

Savio D, Sinclair L, Ijaz UZ, Parajka J, Reischer GH, Stadler P, Blaschke AP, Blöschl G, Mach RL, Kirschner AK (2015) Bacterial diversity along a 2600 km river continuum. Environ Microbiol 17:4994–5007

Schloss PD, Westcott SL, Ryabin T, Hall JR, Hartmann M, Hollister EB, Lesniewski RA, Oakley BB, Parks DH, Robinson CJ (2009) Introducing mothur: open-source, platform-independent, community-supported software for describing and comparing microbial communities. Appl Environ Microbiol 75:7537–7541

Schumacher BA (2002) Methods for the determination of total organic carbon (TOC) in soils and sediments. Ecol Risk Assess Support Cent U.S Environmental Protection Agency, Washington, DC

Segata N, Izard J, Waldron L, Gevers D, Miropolsky L, Garrett WS, Huttenhower C (2011) Metagenomic biomarker discovery and explanation. Genome Biol 12:1–18

Staley C, Unno T, Gould T, Jarvis B, Phillips J, Cotner J, Sadowsky M (2013) Application of Illumina next generation sequencing to characterize the bacterial community of the upper Mississippi River. J Appl Microbiol 115:1147–1158

Straub KL, Benz M, Schink B (2001) Iron metabolism in anoxic environments at near neutral pH. FEMS Microbiol Ecol 34:181–186

Sun M, Xiao T, Ning Z, Xiao E, Sun W (2015a) Microbial community analysis in rice paddy soils irrigated by acid mine drainage contaminated water. Appl Microbiol Biotechnol 99:2911–2922

Sun W, Xiao E, Dong Y, Tang S, Krumins V, Zengping N, Sun M, Zhao Y, Wu S, Xiao T (2016) Profiling microbial community in a watershed heavily contaminated by an active antimony (Sb) mine in Southwest China. Sci Total Environ 550:297–308

Sun W, Xiao T, Sun M, Dong Y, Ning Z, Xiao E, Tang S, Li J (2015b) Diversity of the sediment microbial community in the Aha watershed (Southwest China) in response to acid mine drainage pollution gradients. Appl Environ Microbiol 81:4874–4884

Tamura H, Goto K, Yotsuyanagi T, Nagayama M (1974) Spectrophotometric determination of iron (II) with 1,10-phenanthroline in the presence of large amounts of iron (III). Talanta 21:314–318

Templeton AS, Staudigel H, Tebo BM (2005) Diverse Mn (II)-oxidizing bacteria isolated from submarine basalts at Loihi Seamount. Geomicrobiol J 22:127–139

Vile MA, Wieder RK (1993) Alkalinity generation by Fe (III) reduction versus sulfate reduction in wetlands constructed for acid mine drainage treatment. Water Air Soil Pollut 69:425–441

Wang Q, Garrity GM, Tiedje JM, Cole JR (2007) Naive Bayesian classifier for rapid assignment of rRNA sequences into the new bacterial taxonomy. Appl Environ Microbiol 73:5261–5267

Zhang N, Wan S, Li L, Bi J, Zhao M, Ma K (2008) Impacts of urea N addition on soil microbial community in a semi-arid temperate steppe in northern China. Plant Soil 311:19–28

Ziegler S, Waidner B, Itoh T, Schumann P, Spring S, Gescher J (2013) *Metallibacterium scheffleri*, gen. nov., sp. nov., an alkalinizing gammaproteobacterium isolated from an acidic biofilm. Int J Syst Evol Microbiol 63:1499–1504